Open Research Online

The Open University's repository of research publications
and other research outputs

Macroscopic Characterization of Mechanical Properties in Electric Current Treated Dry Drawn High Strength Wires

Journal Item

How to cite:

Omoigiade, Osamudiamen; Haldar, Arunansu and Qin, Rongshan (2017). Macroscopic Characterization of Mechanical Properties in Electric Current Treated Dry Drawn High Strength Wires. MRS Advances, 2(17) pp. 963–974.

For guidance on citations see FAQs.

© 2017 Materials Research Society

https://creativecommons.org/licenses/by-nc-nd/4.0/

Version: Accepted Manuscript

Link(s) to article on publisher's website:
http://dx.doi.org/doi:10.1557/adv.2017.182

Copyright and Moral Rights for the articles on this site are retained by the individual authors and/or other copyright owners. For more information on Open Research Online's data policy on reuse of materials please consult the policies page.

oro.open.ac.uk

Macroscopic Characterization of Mechanical Properties in Electric Current Treated Dry Drawn High Strength Wires

Osamudiamen Omoigiade[1], Arunansu Haldar[2], and Rongshan Qin[3,1]

[1]*Department of Materials, Imperial College London Exhibition Road, London SW7 2AZ, UK*
[2]*TATA Steel Swinden Technology Centre, Moorgate, Rotherham S60 3AR, UK*
[3]*School of Engineering I& Innovation, The Open University, Milton Keynes MK7 6AA, UK*

ABSTRACT

The present paper investigates the use of electric current treatment in improving the drawability of plain carbon steel wire for high strength steel applications. The mechanical properties for wires of composition 0.80C 0.65Mn 0.27Si wt.% of diameters 4.09 and 3.00 mm dry drawn from 10.00 mm rods are characterised. The total number of passes for 4.09 and 3.00 mm diameter wires are 7 and 10 respectively resulting in true strains of 1.79 and 2.41. Samples are treated with electric currents in-between the two drawing stages of 4.09 and 3.00 mm, and tested at both stages in tension, torsion and reverse bending along with control samples for comparison. The applied currents are pulsed at a frequency of 100 Hz with each pulse being approximated by a square wave of loading width $80\mu s$ and modest current densities of 7.96 Amm^{-2}. Thus the influence of electric current on the drawability of plain carbon steel wire is assessed between stages of reduction.

INTRODUCTION

High strength steel wires are used in a range of applications including pneumatic tires in the automotive industry. These are composites of an elastomeric matrix reinforced with steel. These steels have a fully pearlitic microstructure hence exhibit high work hardening rates which enable them to achieve competitive strengths demanded of their applications while retaining sufficient ductility. The strength of the steel is limited by the starting microstructure in particular the pearlite interlamlellar spacing, where a finer spacing results in greater strength [1]. Although the drawing procedure, which is the driving force for work hardening in the microstructure contributes most significantly to strength increases [2]. The drawing procedure is a step by step reduction in wire diameter by pulling the feedstock through holes in drawing dies inlaid with a hard metal carbide to successively smaller diameters.

However, severe drawing distorts the pearlite microstructure which eventually becomes prone to delamination before the target diameter is reached. Delamination is characterised by cracking along the length of a wire such that the wire is no longer in one piece. Types of delamination in steel wire are described in detail by Godecki [3]. In order to circumvent early fracture, the microstructure is restored through a patenting process before conducting wet wire drawing; the third and last wire manufacturing stage precedent to dry drawing and mill-rolling. Whereby the steel is re-austenitized at 900-1000^{o}C and then quenched into a molten salt or lead bath of $\sim 540^o$C to form a fine pearlite microstructure that can be further drawn. Unfortunately this interruption to drawing slows the manufacturing process increases the opportunity cost and lowers output rate. Therefore the ability to have continued reduction of wires, that is, improved ductility and strength without resorting to patenting is a commercially attractive objective for improving wire drawability.

One suggested approach is an in-situ treatment that can permit extended drawing time, and potentially omit the patenting step involving the application of electric current. Since Troistki's 1963 paper [4] on electroplasticity, the theme soared in popularity for almost two decades, and has experienced a recent resurgence

although with revised theoretical understanding the phenomenon's origin [5–7]. The concept was traditionally explained to occur by an increased mobility of dislocations caused by the applied current exerting a composite force on them. This was later disproved and replaced in favor of a more conservative theory attributing the apparent increase in plasticity to a softening of the material caused by transient heating which lead to significant deformations under smaller than expected loads [8]. The transient influence of electric currents on metal deformation has been studied extensively [9–11], however no adequate consideration has been given to the permanent changes in properties caused by this in-situ treatment. Therefore it is of interest to electrically treat cold drawn wire, between different stages of drawing to determine non-transient effects of electric current treatment on the properties of drawn wire and determine whether these effects are beneficial or deleterious in light of the enhanced plastic deformation presented by electric current treatment.

These properties will be assessed in accordance with industrial standards by considering the mechanical properties of wires under torsion, tensile and reverse bending. The nature of these tests are reflective of the stresses the wires would be subject to during in-service loading as well as during drawing and manufacturing, where in tire cords for example wires are stranded. From the performance of the material in these tests, information about wire drawability can be inferred using data obtained on resistance to uniaxial load and shearing from tensile and torsion tests respectively, as well as reverse bend tests which provides insight into a wire's ductility through a rapid fatigue test. As such, an adequate macroscopic assessment of wire drawability can be achieved, where drawability is synonymous with ductility for the purposes and intents of this work.

EXPERIMENTAL

Materials

In this investigation, five 10.0 mm diameter rods of 300 mm length cut from the same wap of rod (wound bundles of steel rod that have a defined circumference) rolled from the mill were used. The produced rod is a plain carbon steel of composition Fe 0.80C 0.65Mn 0.27Si wt.% confirmed industrially via an iterative chemical analysis involving inductively coupled plasma mass spectrometry. Due to the nature of the forced air cooling treatment during production the starting microstructure of rods from the same wap may vary across the circumference of the wound rod, heat treatments prior to experimental drawing and testing were therefore conducted to improve the microstructural uniformity across individual samples. These involved austenitizing samples at 1000^oC for 8 minutes in a tube furnace, followed by a forced air cooling treatment. K-type thermocouples were physically inserted into drilled holes at the ends of the rods forming an intimate contact enabling temperature profiles detailing the endothermic austenitization and exothermic pearlite transformation as well as the holding time during austenitization (Figure 1).

Drawing Procedure

After heat treatment, samples were de-scaled and phosphate coated in preparation of the dry drawing procedure. All five samples underwent 7 passes, reducing the diameter from 10.0 mm to 4.09 mm. After which the wires were divided into two groups, the first comprising of samples which would be tested at 4.09 mm and the second group of samples that would be drawn further to 3.00 mm. The drawing procedure is detailed in Table 1. As a result of conservation of mass, the wires of reduced diameter have significantly increased lengths, allowing sample lengths which satisfy industry standards to be used in each kind of mechanical test. Group 1 consists of three repeats 1a, 1b and 1c which have been drawn from 10 mm to 4.09 mm. Each repeat had half its samples electrically treated post-drawing while the rest remained untreated in an as drawn condition as control specimens and both were subsequently mechanically tested. Samples in Group 2 also consists of three repeats of 2a, 2b and 2c. These were initially drawn to 4.09 mm and likewise, had half electrically treated while the rest were left in the as drawn condition as control specimens. After which all Group 2 samples were drawn a further 3 passes reducing samples to diameters of 3.00 mm and then mechanically tested.

The samples in Group 1 and 2 were drawn to a true strain of 1.79 and 2.41 at diameters of 4.09 mm and 3.00 mm respectively. Since samples were drawn from large diameters to smaller diameters, the increased lengths of the rods were adequate to carry out mechanical testing while avoiding use of material near the

pointed end of the specimen or at the rear, whose mechanical properties are likely to deviate from those in the wire's central region due to differences in heat generated in these areas during drawing.

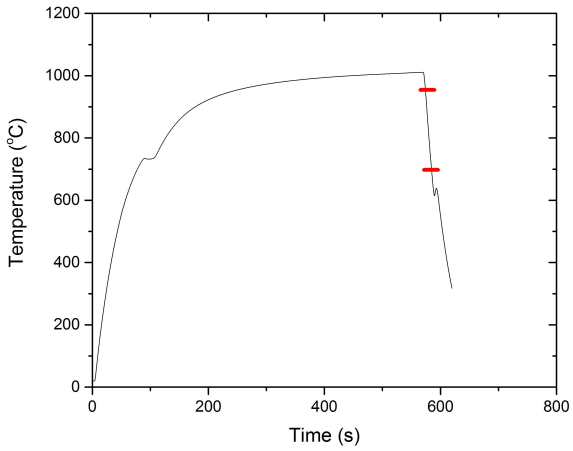

Figure 1: Temperature profile for the prior heat treatment of sample 1b as a 10 mm rod. Pearlite cooling rates were calculated from region marked on profile using OriginPro.

Electric Current Treatment

The application of the electric current to treat samples was achieved by using copper wires attached to a current generator, AVTECH model AV-108F-2-B-P powered by a Delta Electronika SM1500 series SM 35-45 DC power supply. The nature of the current applied is an AC current, with a DC offset oscillating between a positive potential and zero, not becoming negative at any point. Their form is approximately a square wave and they are pulsed at frequencies of 100 Hz and have loading widths of 80 μs of current amplitudes 100 A, supplied by a DC potential of 24 V. The current is applied for 10 minutes to each of the treated samples.

To determine the increase in temperature of samples during electric current treatment, K-type thermocouples were spot welded on to the surface of rods at equidistant positions. Temperature change with time was monitored using a multichannel picologger, from which a temperature profile across the length of the sample could be mapped (Figure 2). There were measurable temperature increases for samples subject to electric current pulses at room temperature. Identical electric current parameters were used in the sample treatment for drawn wires to those in the temperature measurement experiments.

Table 1: Experimental drawing procedure applied to rods reduced from 10 mm diameter to 4.09 mm diameter and 3.00 mm.

Pass No	Diameter of Die (mm)	Total Strain intensity (€)	Surface Area Reduction ratio	Incremental Reduction of Area (%)	Cumulative Reduction of Area (%)
Initial	10.00	-	-	-	-
1	8.83	0.25	0.78	22.05	22.05
2	7.80	0.50	0.61	21.95	39.16
3	6.83	0.76	0.47	23.33	53.35
4	6.01	1.02	0.36	22.57	63.88
5	5.29	1.27	0.28	22.52	72.02
6	4.68	1.52	0.22	21.73	78.10
7	4.09	1.79	0.17	23.62	83.27
8	3.68	2.00	0.14	19.04	86.46
9	3.30	2.22	0.11	19.59	89.11
10	3.00	2.41	0.09	17.52	91.02

Mechanical Testing

Torsion

Specimen gauge lengths of 204.5 mm and 149.85 mm were used to test wires of 4.09 mm and 3.00 mm diameter respectively. Test were conducted using the Instron Torsion machines 55MT2 in accordance with testing standard BS ISO 7800. Rotations were performed at a rate of 30 revolutions per minute (rev/min) for both wire diameters, although different dead loads were used, 45 kg for 4.09 mm and 30 kg for 3.00 mm. The torsion cell in this apparatus is a flanged reaction torque transducer, enabling higher resistance to bending moments and has high torsional stiffness, particularly advantageous for large test pieces with relatively high stiffness as with the drawn carbon steel wires considered in this experiment. Tests were conducted at room temperature.

Tensile

Wire specimens of circular cross section and diameters of 4.09 and 3.00 mm with a gauge length of 50 mm were tensile tested in an Instron 300DX Tensile Machine using a 300 kN load cell in accordance with testing standard BS EN ISO 6892-1. Samples are extended at room temperature with a constant cross head speed of 5 mm min^{-1}. Carbon steel wires exhibited upper and lower yield points, and the 0.2% proof stress was determined using a 25 mm gauge length extensometer attached to the samples whose values were consistently below the first yield point (upper). Reference will be made to yield stress where necessary, however focus will be placed on ultimate tensile strength (UTS) and 0.2% proof stress when comparing results.

Reverse Bending

Reverse bends over radius grips subject to cyclic loading fatigue tests were performed in a Hegewald and Peschke Reverse Bend Tester according to testing standard ISO7801. Specimens of diameter 4.09 mm and 3.00 mm, treated with electric current and without were subject to bends which deflected the sample 90^o about the radius grips at a nominal frequency of 1 Hz in room temperature environment in air. The lower end of the test specimen was clamped into rigid holder and fed through a pair of rolls. The top end of the specimen was clamped in a movable, motor-driven bending arm which applied the force. The positioning of the pair of rolls enabled bending to take place at discrete positions along the length of the rod depending on the diameter in accordance with standards. The cyclic bending involved bending the sample to the left, 90^o and then to the right, 180^o until sample fracture.

Electron Microscopy

Secondary electron images of the fracture surfaces of samples were obtained using a JSM6010LV. The tall chamber is ideal for obtaining a working distance suitable for taking low magnification images of large objects in a wide field of view. The microscope was operated at accelerating voltage 20kV and working distance of approximately 50 mm. Image magnifications of x23 and x17 were used to image flat fracture surfaces on wires 3.00 mm and 4.09 mm respectively. Samples with angular fracture were imaged at x10 magnification for both sample diameters. For samples where both angular and flat fractures occur, flat fracture fractographs were included as an inset image in the corresponding sample figure.

RESULTS

Temperature Change with Electrical Current Treatment

The temperature profile in Figure 2 shows an average increase of 25^oC in the sample from room temperature to $\sim 50^o$C, with an apparent minimum near the centre of the sample. This arises due to the bi-metallic junction between the copper wire and the steel wire, resulting in a heat exchange on account of their dissimilar Peltier coefficients. In this experiment, thermocouples welded to junctions at the ends of the sample were close to the attached copper wire, hence the increase in temperature due to the bi-metallic junction is accordingly detected by these thermocouples at the wire extremities.

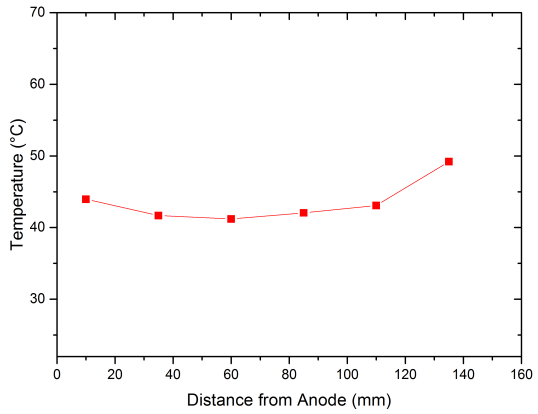

Figure 2: Temperature profile across length of a plain carbon wire with pulsed electric current passing through it at a frequency of 100 Hz with a loading width of 80 μs and current 100 A.

Mechanical Testing

Tensile Testing

The reported tensile curves are generally representative of those observed for samples tested at diameters 4.09 mm and 3.00 mm as shown in Figure 3A and B respectively. These compare the behaviour of electric current treated specimens in tension. The tabulated values of the UTS and 0.2% proof stress in Table 2 show a consistent increase for electric current treated samples in comparison to those which did not receive treatment. This observation remains the same for both sample diameters. There is also a notable decrease in % tensile elongation in Figures 3A and B for electric current treated samples of approximately 0.5% suggesting loss of ductility.

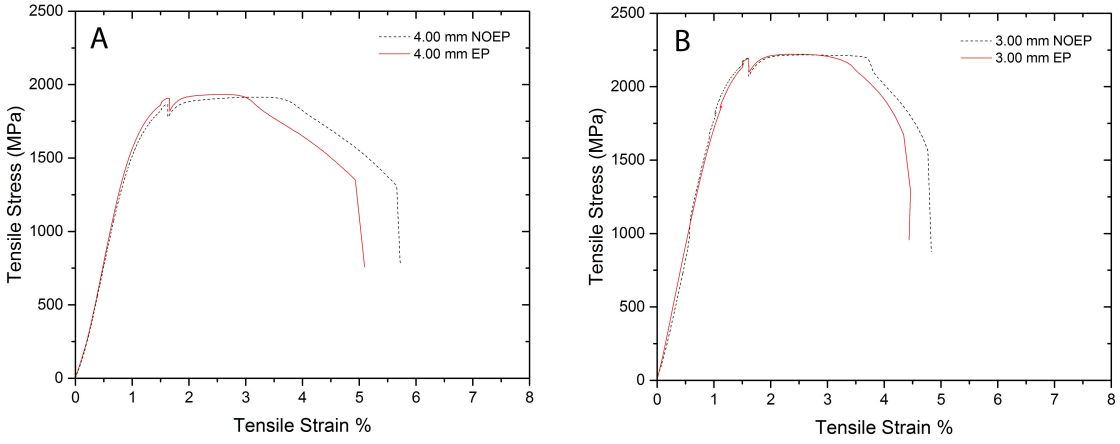

Figure 3: Tensile plots of specimens with electric current treatment at 4.09 mm and without at testing diameters of (A) 4.09 mm and (B) 3.00 mm.

Table 2: Mechanical properties in tension, torsion and reverse bending corresponding to specific test specimens.

Sample	Drawing Strain (ε)	Testing Diameter (mm)	Cooling Rate (°C/s)	Current Treatment				UTS (Mpa)	0.2% Proof Stress (MPa)	Max. Shear Stress (MPa)	Max. Shear Strain (γ)	Number of Revolutions to Fracture	Torsion Fracture Type	Number of Bends to Fracture
				Frequency (Hz)	Current Density (A/mm^2)	Voltage (V)	Pulse Width (μs)							
1a	1.79	4.09	28	-	-	-	-	1907	1691	1592	1.060	16.9	1A + 1B	24
1a EP	1.79	4.09	28	100	7.61	24	80	1970	1780	1586	1.268	20.2	1A + 1B	25
1b	1.79	4.09	25	-	-	-	-	1928	1715	1580	0.975	15.5	3A + 3C	23
1b EP	1.79	4.09	25	100	7.61	24	80	1959	1750	1606	0.994	15.8	3A + 3C	24
1c	1.79	4.09	27	-	-	-	-	1915	1705	1606	1.167	18.6	1A	25
1c EP	1.79	4.09	27	100	7.61	24	80	1933	1747	1594	1.227	19.5	1A	24
2a	2.41	3.00	39	-	-	-	-	2244	2076	1907	0.800	12.7	3A	12
2a EP	2.41	3.00	39	100	7.61	24	80	2305	2097	1988	0.809	12.9	3A + 3C	12
2b	2.41	3.00	26	-	-	-	-	2183	1984	1867	1.031	16.4	3A + 3C	12
2b EP	2.41	3.00	26	100	7.61	24	80	2256	2075	2015	0.871	13.9	3A + 3C	11
2c	2.41	3.00	26	-	-	-	-	2137	1931	2087	0.925	14.7	3A	10
2c EP	2.41	3.00	26	100	7.61	24	80	2186	2046	1935	0.862	13.7	3A + 3C	13

Torsion Testing

The observed reduction in tensile elongation at testing diameters 4.09 mm and 3.00 mm somewhat contrast measured shear strain values for 4.09 mm samples tested in torsion. There was an improvement in ductility (increase in mean maximum shear strain) for electric current treated samples tested at 4.09 mm, and a loss of ductility for those tested at 3.00 mm (Figure 4). However, shear strain values can be variable due its sensitivity to surface quality. The drop in shear stress in Figure 4B signals the onset of delamination in the wire, which occurred in both electric current treated samples and non-treated samples at 3.00 mm. With the largest changes in maximum shear strain for group 1 and 2 being a 19.6% increase in sample 1a and 15.5% decrease in sample 2b (Table 2).

The maximum measured shear stress is variable between samples treated with electric current and those without, which is evident from the plotted mean maximum shear stress values obtained for both wire diameters in Figure 5. Indicating nominal changes for specific experiments are not statistically significant and the shear stress remains unchanged with treatment. That notwithstanding, there was predictably an increase in maximum shear stress with increased drawing strain as observed in samples with strain 2.41, at which a higher UTS and 0.2% proof stress was also observed in agreement with increased cold work [2]. All error bars shown in Figures 5A and B are defined as the standard deviation from the sample mean.

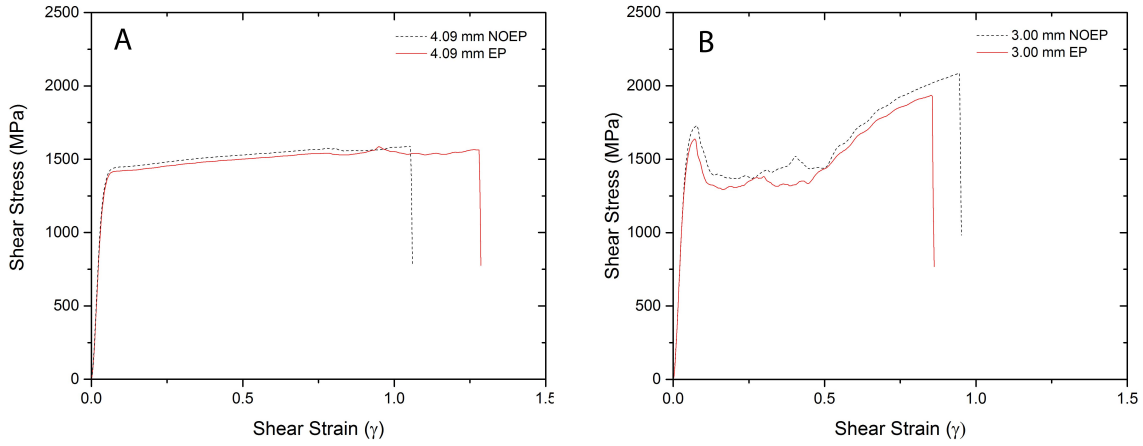

Figure 4: Torsion plots of specimens with electric current treatment at 4.09 mm and without, at testing diameters of 3.00 mm and 4.09 mm.

Generally the mean UTS has increased with drawing strain, though more pronouncedly in the case of those treated with electric current which recorded higher UTS at 4.09 mm and 3.00 mm. There is an increase in mean UTS in the electric current treated samples of 1.9% for samples tested at 4.09 mm and a marginally higher increase for those tested at 3.00 mm of 2.8%.

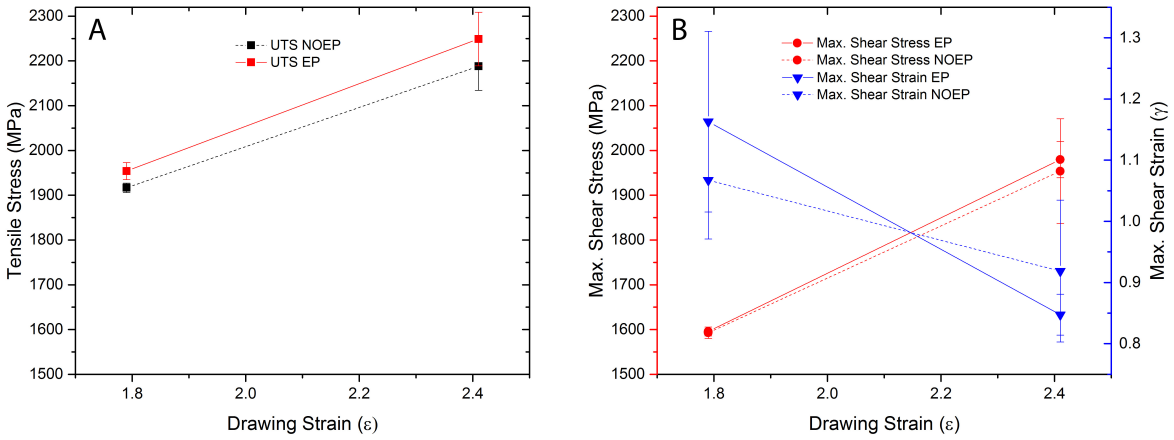

Figure 5: (A)Mean ultimate tensile strength (UTS) values for samples tested at 4.09 mm and 3.00 mm comparing with and without electrical treatment. (B) Analogous plots for the mean maximum shear stress and strain.

Fractographs were obtained for torsion samples treated with electric current and those without. In cases where samples fractured in two positions, both were accordingly imaged and their fracture types indicated in Figures 6 and 7 as well as being listed in Figure 5. A qualitative alpha-numerical scale is used in identifying the fracture surface in this macroscopic study from which the nature of failure can be inferred. The numerical values in the scale indicate the severity of twist and cracking along fissures of the twisted material. Where the following listed numbers indicate 1: Slight twisting with no crack formation; 2: Moderate twisting with crack propagation which is superficial and has not propagated to the centre; 3: Extreme twisting with intensive cracking which has propagated from the surface to the centre causing visible delamination. The letter codes indicate the nature of the fracture surface. The letter codes bare the following significance, A: Flat fracture surface approximately parallel to the twisting direction; B: Angular fracture surface that is non-parallel to twisting direction; C: Angular fracture non-parallel to the twisting direction, with a propagated crack through the twist symmetry axis.

Samples tested at diameters of 4.09 mm exhibit similar fracture surfaces for those with electric current treatment and without as shown in Figure 6. For samples tested at 3.00 mm (Figure 7) there is some indication that the nature of the fractures of electric current treated samples are more brittle as C type surfaces are more common among them. The extents of twisting for samples tested at 3.00 mm are all coded as 3, reflective of the higher maximum shear stress at failure. Flat fracture surfaces coded A, are generally more ductile than angular fracture surfaces such as C.

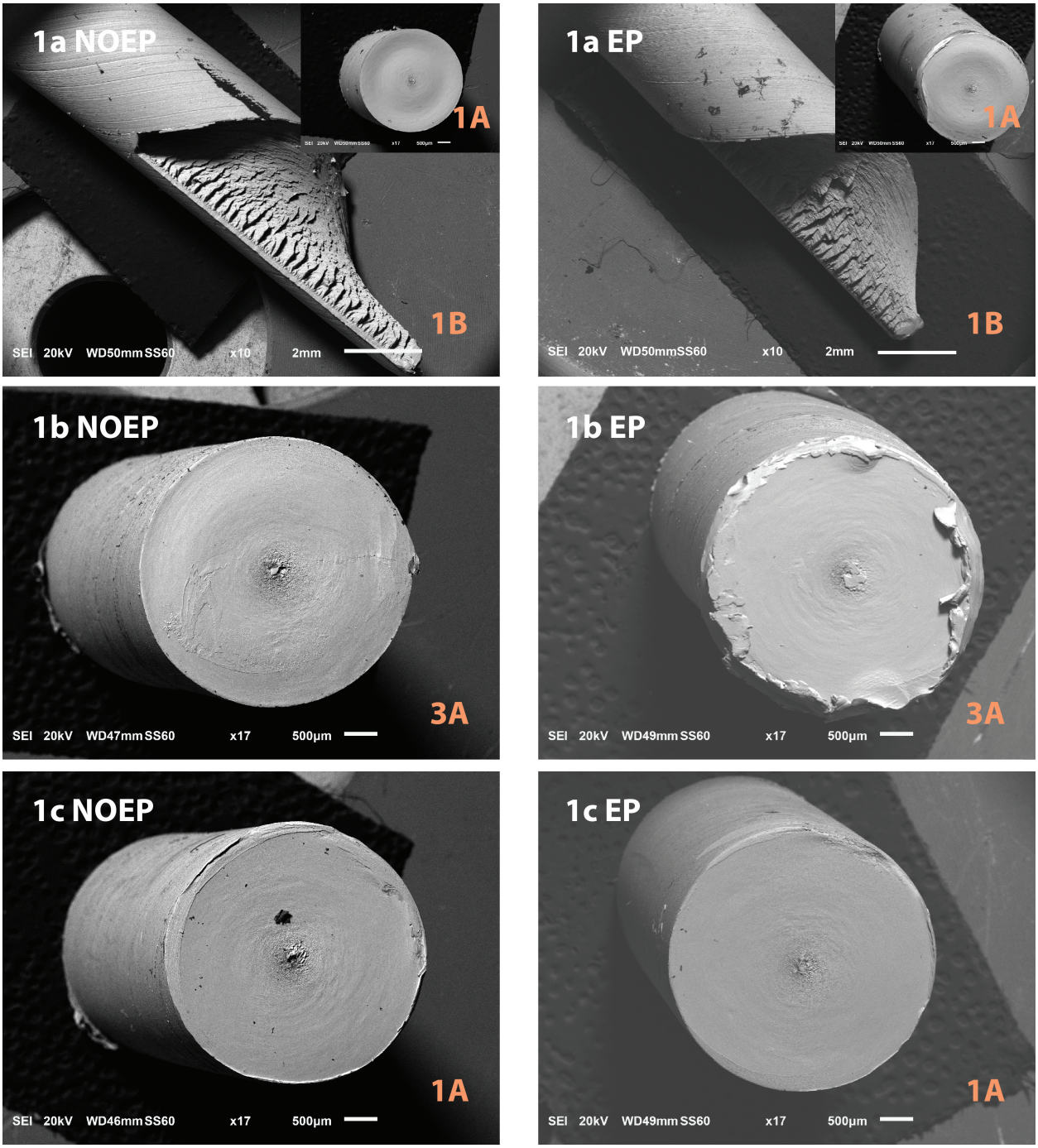

Figure 6: Fracture surfaces of 4.09 mm wire tested in torsion. Those with electric current treatment prior to torsion testing are identified by the code EP, and those without NOEP. The alpha-numeric fracture type are indicated on bottom right corner of each image.

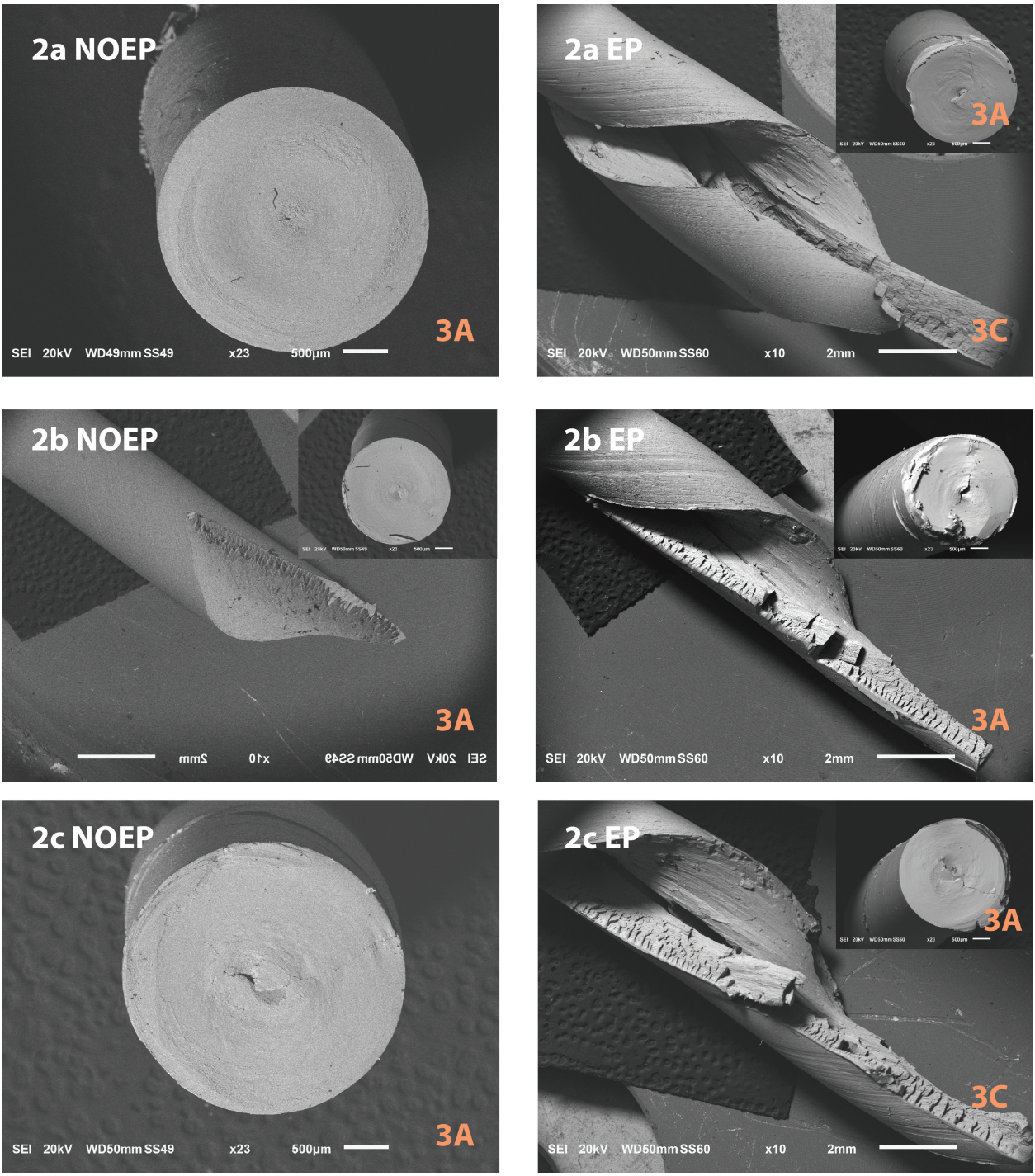

Figure 7: Fracture surfaces of 3.00 mm wire tested in torsion. Those which were treated with electric current at 4.09 mm and afterwards drawn to 3.00 mm are coded EP, and those that were not treated NOEP.The alpha-numeric fracture type are indicated on bottom right corner of each image.

Reverse Bend Tests

The number of reverse bends to failure remains approximately the same for electric current treated samples and those non-treated, the fractographs provided in Figure 8 are representative of the fracture surfaces in

both groups of wire. There is however a noticeable reduction in the number of bends to failure with increased drawing strain, expected of the lower capacity for ductility after drawing. The fracture surfaces in 3.00 mm samples are indicative of a more brittle fracture as seen from the delamination and angular fracture, when compared with the fibrous fracture surfaces in Figure 8A. This is moreover characterised by a necking-type ductile fracture, which showed a 28.6% reduction in diameter, in comparison to null, for the sample tested at 3.00 mm. 4.09 mm samples also had a thin layer of oxide form around the fracture region (which cannot be viewed from the electron micrograph) giving rise to a blue hue on account of heat dissipation in this region.

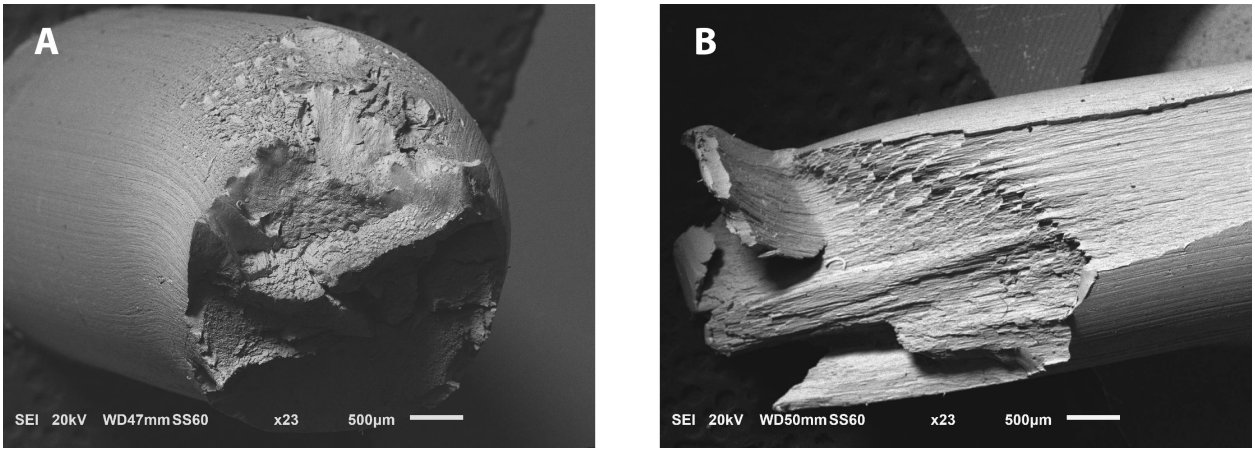

Figure 8: Fracture surfaces for wires of diameter 4.09 and 3.00 mm subject to reverse bending about radius grip at a frequency 1 hz.

DISCUSSION

For the given electric current parameters considered in this investigation reverse bending and measured shear stresses generally appear unchanged. Shear strain values at both considered diameters and torsion fractographs at 3.00 mm show some responsiveness to treatment in the way of reduced ductility. Tensile properties however appear the most sensitive to the treatment, experiencing increases in strength indicated by UTS and 0.2% proof stress increases with reduced elongation to failure.

Between 4.09 mm and 3.00 mm wires there was a decrease in the number of reverse bends to failure and a shift towards less ductile fracture surfaces. These observations appear to be dependent on the amount of cold work in the material, and sample geometry. This is anticipated by the necessarily larger area moment of inertia in sample 4.09 mm dictating it would have a larger resistance to bending. This greater resistance generated more heat in the sample during testing, and may explain the more ductile fracture surface due to a warmer deformation. The reverse bend test, as mentioned previously is a rapid fatigue test, and the results indicate there is no apparent macroscopic change in fatigue resistance with electric current treatment.

Torsion failure modes for sample diameter 4.09 mm are identical for electric current treated samples as for untreated. There is however some difference between sets of samples within group 1, suggesting they are linked to material properties whose variation is influenced by the cooling rate of the starting samples prior to drawing which had some differences. The majority of mechanical properties in pearlite are dictated by the interlamellar spacing, which reduces with higher cooling rates (larger undercooling) [1].

Increases in mean maximum shear strain for electric current treated 4.09 mm samples indicates some recovered ductility. The measured mean maximum shear strain for the electric current treated sample falls below that of the non-treated after further drawing. This is likely due to electric current treatment causing a change in the sensitivity in mechanical properties subject to further deformation which is most aptly described by dynamic strain ageing. The strain ageing kinetics are therefore likely altered by application of the current causing a reduction in a failure strain after being drawn to 3.00 mm.

Tensile strengths responded positively to electric current treatment, in that increases in UTS and yield

strengths increase were recorded; the source of this increase is majorly due to static strain ageing with a minor potential contribution from dynamic strain ageing. The source of the initial static strain ageing for the electric current treated 4.09 mm sample is reasonably the $\sim 50^oC$ (Figure 2) increase in temperature during electric current treatment for a duration of 10 minutes (600 sec). In work by Buono [12], pearlite wire of similar composition 0.82C 0.7Mn 0.23Si wt.% were drawn to a true strain of 2.0 and aged at 60^oC for 400 and 900 seconds experiencing a percentage increase in yield strength of 1 and 1.4% respectively. Analogously, lower yield strengths in this study showed percentage increases of 2.4% for sample 4.09 mm (true strain of 1.79) which is thought to have undergone static strain ageing. Lower yield stress values are used in this comparison as they are typically quoted as engineering yield stresses in steels exhibiting yield drop.

The mean UTS for electric current treated samples are higher at each drawing stage assessed, where an increase of 1.9% and 2.8% was recorded for drawing strains of 1.79 and 2.41 respectively. A result reflected in the respective work hardening rates calculated from the curves in Figure 5A for electric current treated and non-treated samples of 438 and 476 MPa per unit of strain. This remarks a chnage normally achievable by an increase in carbon content of 0.15 wt.% [13]. Tarui [13], observed an increase in work hardening rate of 45 MPa per unit strain in a 0.8wt.% high carbon wire for an increase of .15wt.% C, which is comparable to the 40 MPa per unit strain increase observed for electric current treated wire. It is therefore hypothesised that the increased rate of work hardening arises from increased availability of carbon atoms in solution that has augmented dynamic strain ageing kinetics. Above 1.5 true strain cementite in pearlite begins to dissolve [14], as such for samples strained to 1.79 we assume carbon has begun to dissolve into the ferrite. Therefore the application of current treatment is thought to enhance this dissolution process increasing the carbon atoms in the ferrite. As a result, during further drawing from 4.09 mm to 3.00 mm the dislocations generated experience resistance from carbon atoms as they attempt to slip in response to the applied stress, manifesting an augmented increase in strength in the electric current treated 3.00 mm wire, although further investigation is required to confirm this hypothesis.

CONCLUSION

Tensile properties are shown to be the most sensitive of measured parameters to electric current treatment where notable increases in UTS, work hardening rates and 0.2% proof stress were observed. Reverse bend and maximum shear stress appear invariable to treatment although shear strain shows some recovery of ductility with initial treatment but enhanced kinetics of dynamic strain ageing thereafter leading to lower fracture at lower strains than observed in untreated samples. Electric current treatment for the considered parameters appears to be deleterious to drawing as it increases stresses in the wire through ageing and reduces ductility making drawing more difficult and resulting properties less desirable. Although it does improve strength it does so at the cost of ductility which is important in the drawing process.

ACKNOWLEDGEMENTS

This work was possible thanks to the financial support gained from the Engineering and Physical Sciences Research Council and TATA Steel (Funding number 1322018). Particular thanks to Ian Letchford, Paul Bradley and Shaun Hobson of British Steel Ltd for their invaluable discussions.

References

[1] O. Modi, N. Deshmukh, D. Mondal, A. Jha, A. Yegneswaran, H. Khaira, Effect of interlamellar spacing on the mechanical properties of 0.65% C steel, Materials Characterization 46 (5) (2001) 347–352.

[2] J. Embury, R. Fisher, The structure and properties of drawn pearlite, Acta Metallurgica 14 (2) (1966) 147–159.

[3] L. Godecki, The delamination of spring wires during torsion testing, Wire Ind 7 (1969) 47–51.

[4] O. Troitskii, V. Likhtman, The anisotropy of the action of electron and gamma radiation on the deformation of zinc single crystals in the brittle state, in: Soviet Physics Doklady, Vol. 8, 1963, p. 91.

[5] K. Mori, S. Maki, Y. Tanaka, Warm and Hot Stamping of Ultra High Tensile Strength Steel Sheets Using Resistance Heating, CIRP Annals - Manufacturing Technology 54 (1) (2005) 209–212.

[6] Y. Jiang, G. Tang, C. Shek, Y. Zhu, Z. Xu, On the thermodynamics and kinetics of electropulsing induced dissolution of Mg17Al12 phase in an aged Mg-9Al-1Zn alloy, Acta Materialia 57 (16) (2009) 4797–4808.

[7] R. Delville, B. Malard, J. Pilch, P. Sittner, D. Schryvers, Microstructure changes during non-conventional heat treatment of thin NiTi wires by pulsed electric current studied by transmission electron microscopy, Acta Materialia 58 (13) (2010) 4503–4515.

[8] P. Goldman, L. Motowidlo, J. Galligan, The absence of an electroplastic effect in lead at 4.2K, Scripta Metallurgica 15 (4) (1981) 353–356.

[9] K. Okazaki, M. Kagawa, H. Conrad, A study of the electroplastic effect in metals, Scripta Metallurgica 12 (11) (1978) 1063–1068.

[10] A. Sprecher, S. Mannan, H. Conrad, On the mechanisms for the electroplastic effect in metals, Acta Metallurgica 34 (7) (1986) 1145–1162.

[11] H. Conrad, Effects of electric current on solid state phase transformations in metals, Materials Science and Engineering: A 287 (2) (2000) 227–237.

[12] V. T. L. Buono, B. M. Gonzalez, M. S. Andrade, Kinetics of strain aging in drawn pearlitic steels, Metallurgical and Materials Transactions A 29 (5) (1998) 1415–1423.

[13] T. Tarui, J. Takahashi, H. Tashiro, N. Maruyama, S. Nishida, Microstructure Control and Strengthening of High-carbon Steel Wires, Nippon Steel Tech. Report (91) (2005) 56–61.

[14] A. Lamontagne, V. Massardier, X. Klber, X. Sauvage, D. Mari, Comparative study and quantification of cementite decomposition in heavily drawn pearlitic steel wires, Materials Science and Engineering: A (2015) 105–113.